

Research Article

On Reverse Valency Based Topological Characterization of a Chemical Compound

Maria Singaraj Rosary¹ and Samuel Asefa Fufa ²

¹Department of Mathematics, Vel Tech High-Tech Dr. Rangarajan Dr. Sakunthala Engineering College, Chennai 600062, India

²Department of Mathematics, Addis Ababa University, Addis Ababa, Ethiopia

Correspondence should be addressed to Samuel Asefa Fufa; samlen2006@yahoo.com

Received 14 March 2022; Revised 27 June 2022; Accepted 11 July 2022; Published 11 August 2022

Academic Editor: Mehar Ali Malik

Copyright © 2022 Maria Singaraj Rosary and Samuel Asefa Fufa. This is an open access article distributed under the Creative Commons Attribution License, which permits unrestricted use, distribution, and reproduction in any medium, provided the original work is properly cited.

Metal-organic frameworks explicit the consequence of these frameworks with adjustable implementations, namely, energy storage gadgets of magnificent electrode materials, gas store, heterogeneous catalysis, environmental hazard, estimation of chemicals, recognizing of definite gases, controlling solids, and supercapacitors. In this paper, we give explicit expression of the reverse general Randic index, the reverse atom bond connectivity index, the reverse geometric arithmetic index, the reverse forgotten index, the reverse Balaban index, the reverse augmented index, and different types of reverse Zagreb indices of the metal-organic framework M1TPyP-M2 (TPyP = 5, 10, 15, 20-tetrakis (4-pyridyl) porphyrin and M1, M2 = Fe and Co). A graphical comparison of the calculated different types of the reverse degree based topological indices with the aid of the numerical values is also included.

1. Introduction

Metal-organic frameworks (MOFs) are valuable in modern chemistry. They are described by their three-dimensional frameworks constructed of metal ions and organic molecules. Chu et al. studied the topological indices of MOFs [1]. Certain topological descriptors of certain metal-organic frameworks are well studied in 2020 [2]. In 1959, the initial metal-organic framework was described by Kinoshita et al. [3]. Metal-organic frameworks acquire a great observation required to the work of reticular chemistry for their synthesis [4]. Later, millenarian of MOFs came to be synthesized and widen the range of their prospective applications. Metal-organic frameworks have exhibited applications in the domain of gas catalysis [5], drug delivery [6], and storage [7].

Let $G(V(G), X(G))$ be an ordered pair of graphs, where $V(G)$ is a nonempty vertex set and $X(G)$ is an edge set. A molecular graph is a set of points denoting the atoms in the molecule and collection of lines denoting the covalent bonds. The topological descriptors are helpful in the forecast of physical and chemical properties and the bioactivity of

chemical compounds [8, 9]. They are playing a very important role in the field of chemistry.

Topological indices are important tools for investigating many physicochemical properties of molecules without performing any testing. They are also used to study Quantitative Structure Activity Relationship (QSAR) of pharmaceuticals to determine their molecular characteristics by numerical computation [10]. Various types of topological indices of graphs are classified into distance-based topological indices, degree-based topological indices, and spectrum-based topological indices. Among these, degree-based topological indices play a vital role in theoretical chemistry and pharmacology. Some important degree-based indices are Randic index, Zagreb indices, Harmonic index, and sum connectivity index. For example, Randic index is one of the excellent molecular descriptors in (QSAR) studies and is desirable for measuring the extent of branching of the carbon-atom skeleton of saturated hydrocarbons [11]. The atom-bond connectivity (ABC) index yields a good representation for the stability of linear and branched alkanes as well as the strain energy of cycloalkanes. For particular

physical chemical properties, the diagnostic power of GA index is better than the diagnostic power of the Randić connectivity index [12]. Zagreb-type indices relieved to differentiate some alkane isomers boiling points and have aided in the invention, along with other indices, of a few thousand topological graph indices accepted in the chemical databases [13]. There are a number of research studies on the Zagreb indices and their chemical applications [14].

In chemical graph theory, a topological index predicts the biological activity of the molecular graph of chemical compounds [15]. At first, Wiener gave the idea of topological indices during his work on the boiling point of paraffin and mentioned it as “Wiener index,” an initial topological index. In the literature, the most widely used topological indices are Zagreb and Randić [16, 17]. Recently, the topological indices on product graphs and the inverse sum index of hyaluronic acid-paclitaxel molecules applied in anticancer drugs are extensively discussed [18, 19]. Second Zagreb indices of transformation graphs and total transformation graphs and topological indices on hex-derived networks are presented in [20, 21].

The degree of vertex p in a graph is the total number of edges incident with vertex p , and it is denoted by $\chi(p)$. A graph can be explained by numerical value, matrix, and polynomial. The concept of reverse vertex degree $\mathfrak{R}(p) = \Delta(G) - \chi(p) + 1$ was given by Kulli [22]. In a graph, the maximum degree of the vertex is given by $\Delta(G)$. Degree-, distance-, eccentric-, and spectrum-based indices are special varieties of topological indices. The computation of topological indices has brought up a wide diversity of dormant uses for the evaluation of (QSAR) antiparasitic products. Reverse degree based molecular descriptors of remdesivir used in the treatment of coronavirus are discussed in [23].

Recently, the reverse degree based indices of polycyclic metal-organic network were discussed by Zhao et al. [24]. Jung et al. explained the reverse degree based indices of some nanotubes [25]. Reverse degree based molecular descriptors of graphene are discussed in [26]. Reversed degree based topological indices of benzenoid systems are extensively studied in [27]. Recently, Rosary and Liu presented the reverse degree based topological analysis on the line graph and paraline graph of remdesivir used for the treatment of coronavirus [28, 29]. In this article, we examine the physical chemical properties and the biological activity of the molecular structure of the metal-organic framework M1TPyP-M2. Also, we discuss the reverse degree based topological indices of the metal-organic framework M1TPyP-M2 and compare the results graphically.”

Milan Randić introduced the first degree based index [17]. Wei et al. defined the reverse Randić index as [23]

$$\widehat{\mathfrak{R}}_{\alpha}(G) = \sum_{pq \in X(G)} [\widehat{\mathfrak{R}}_{\chi}(p) \times \widehat{\mathfrak{R}}_{\chi}(q)]^{\alpha}; \quad \alpha = 1, -1, \frac{1}{2}, -\frac{1}{2}. \quad (1)$$

Estrada et al. presented the atom bond connectivity index [30]. Wei et al. defined the reverse atom bond connectivity index as [23]

$$\widehat{\mathfrak{R}}_{ABC}(G) = \sum_{pq \in X(G)} \sqrt{\frac{\widehat{\mathfrak{R}}_{\chi}(p) + \widehat{\mathfrak{R}}_{\chi}(q) - 2}{\widehat{\mathfrak{R}}_{\chi}(p) \times \widehat{\mathfrak{R}}_{\chi}(q)}}. \quad (2)$$

Vukicevic et al. proposed the geometric arithmetic index [31]. Wei et al. defined the reverse geometric arithmetic index as [23]

$$\widehat{\mathfrak{R}}_{GA}(G) = \sum_{pq \in X(G)} \frac{2\sqrt{\widehat{\mathfrak{R}}_{\chi}(p) \times \widehat{\mathfrak{R}}_{\chi}(q)}}{\widehat{\mathfrak{R}}_{\chi}(p) + \widehat{\mathfrak{R}}_{\chi}(q)}. \quad (3)$$

Gutman discussed the first and second Zagreb indices [16, 32]. Wei et al. defined the reverse first and reverse second Zagreb indices as [23]

$$\begin{aligned} \widehat{\mathfrak{R}}_{M_1}(G) &= \sum_{pq \in X(G)} (\widehat{\mathfrak{R}}_{\chi}(p) + \widehat{\mathfrak{R}}_{\chi}(q)), \\ \widehat{\mathfrak{R}}_{M_2}(G) &= \sum_{pq \in X(G)} (\widehat{\mathfrak{R}}_{\chi}(p) + \widehat{\mathfrak{R}}_{\chi}(q)). \end{aligned} \quad (4)$$

Doslic and Gutman et al. [33, 34] presented the first and second Zagreb co-indices. Wei et al. defined the reverse first and reverse second Zagreb co-indices as [23]

$$\begin{aligned} \widehat{\mathfrak{R}}_{\overline{M}_1}(G) &= 2|X(G)|(|V(G)| - 1) - \widehat{\mathfrak{R}}_{M_1}(G), \\ \widehat{\mathfrak{R}}_{\overline{M}_2}(G) &= 2|X(G)|^2 - \frac{1}{2}\widehat{\mathfrak{R}}_{M_1}(G) - \widehat{\mathfrak{R}}_{M_2}(G). \end{aligned} \quad (5)$$

Shirdel et al. [35] discussed hyper Zagreb index. Wei et al. defined the reverse hyper Zagreb index as [23]

$$\widehat{\mathfrak{R}}_{HM}(G) = \sum_{pq \in X(G)} [\widehat{\mathfrak{R}}_{\chi}(p) + \widehat{\mathfrak{R}}_{\chi}(q)]^2. \quad (6)$$

Wei et al. defined the reverse first multiple and the reverse second multiple Zagreb indices as [23]

$$\begin{aligned} \widehat{\mathfrak{R}}_{PM_1}(G) &= \prod_{pq \in X(G)} [\widehat{\mathfrak{R}}_{\chi}(p) + \widehat{\mathfrak{R}}_{\chi}(q)], \\ \widehat{\mathfrak{R}}_{PM_2}(G) &= \prod_{pq \in X(G)} [\widehat{\mathfrak{R}}_{\chi}(p) + \widehat{\mathfrak{R}}_{\chi}(q)]. \end{aligned} \quad (7)$$

Furtula and Gutman [36] introduced forgotten index. Wei et al. defined the reverse forgotten index as [23]

$$\widehat{\mathfrak{R}}_F(G) = \sum_{pq \in X(G)} \left[\widehat{\mathfrak{R}}_{\chi}(p)^2 + \widehat{\mathfrak{R}}_{\chi}(q)^2 \right]. \quad (8)$$

Wei et al. defined the reverse Balaban index for a graph of order q and size p as [23],

$$\widehat{\mathfrak{R}}_J(G) = \frac{p}{p - q + 2} \sum_{pq \in X(G)} \frac{1}{\sqrt{\widehat{\mathfrak{R}}_{\chi}(p) \times \widehat{\mathfrak{R}}_{\chi}(q)}} \quad (9)$$

For a graph, the redefined first, second, and third Zagreb indices are studied in [37]. Wei et al. defined the reverse redefined first, second, and third Zagreb indices as [23]

$$\begin{aligned} \widehat{\mathfrak{R}}\mathfrak{R}_{eZG_1}(G) &= \sum_{pq \in X(G)} \frac{\widehat{\mathfrak{R}}_{\chi}(p) + \widehat{\mathfrak{R}}_{\chi}(q)}{\widehat{\mathfrak{R}}_{\chi}(p) \times \widehat{\mathfrak{R}}_{\chi}(q)}, \\ \widehat{\mathfrak{R}}\mathfrak{R}_{eZG_2}(G) &= \sum_{pq \in X(G)} \frac{\widehat{\mathfrak{R}}_{\chi}(p) \times \widehat{\mathfrak{R}}_{\chi}(q)}{\widehat{\mathfrak{R}}_{\chi}(p) + \widehat{\mathfrak{R}}_{\chi}(q)}, \\ \widehat{\mathfrak{R}}\mathfrak{R}_{eZG_3}(G) &= \sum_{pq \in X(G)} (\widehat{\mathfrak{R}}_{\chi}(p) \times \widehat{\mathfrak{R}}_{\chi}(q)) (\widehat{\mathfrak{R}}_{\chi}(p) + \widehat{\mathfrak{R}}_{\chi}(q)). \end{aligned} \tag{10}$$

Furtula et al. [10] presented augmented Zagreb index. Wei et al. defined the reverse augmented Zagreb index as [23]

$$\widehat{\mathfrak{R}}AZI(G) = \sum_{pq \in X(G)} \left(\frac{\widehat{\mathfrak{R}}_{\chi}(p) \times \widehat{\mathfrak{R}}_{\chi}(q)}{\widehat{\mathfrak{R}}_{\chi}(p) \times \widehat{\mathfrak{R}}_{\chi}(q) - 2} \right)^3. \tag{11}$$

2. Main Results

In order to analyse our results, we use the key technique of combinatorial computing, vertices degree counting, edge dividing scheme, logical techniques, and sum of degrees of neighbors' technique. In addition, we use MATLAB program to do mathematical calculations and plot the results graphically.

The 2-dimensional structure of M1TPyP – M2 MOFs is given in Figure 1. Let $G(p, q)$ be the graph of M1TPyP – M2 MOFs, where p and q are the number of unit cells in each row and column. The 2-dimensional structure of the molecular graph of $G(2, 2)$ is depicted in Figure 1. The cardinality of vertices and edges in M1TPyP-M2 MOFs is $74pq$ and $88pq - 2p - 2q + 1$.

Based on the degree of end vertices, the edges of M1TPyP-M2 MOFs (M1, M2=Fe and Co) can be partitioned into four partitions. The first edge partition includes of $24pq + 1$ edges pq , where $\chi(p) = 1$ and $\chi(q) = 3$. The second edge partition includes of $6p + 6q - 6$ edges pq , where $\chi(p) = 2$ and $\chi(q) = 3$. The third edge partition includes of $56pq - 4p - 4q + 2$ edges pq , where $\chi(p) = 3$ and $\chi(q) = 3$. The fourth edge partition includes $8pq - 4p - 4q + 4$ edges pq , where $\chi(p) = 3$ and $\chi(q) = 4$. Table 1 shows the edge partition of M1TPyP-M2 MOFs.

The maximum degree of the vertex of M1TPyP-M2 MOFs is 4. By using the definition of reverse vertex degree $\mathfrak{R}(p) = \Delta(G) - \chi(p) + 1$, the reverse degree based edge partition of M1TPyP-M2 MOFs is given in Table 2.

Now, we calculate the reverse degree based topological indices as follows.

Theorem 1. We consider the graph $G(p, q)$, then the reverse general Randic index is equal to

$$\widehat{\mathfrak{R}}R_{\alpha}(G(p, q)) = \begin{cases} 416pq + 12(p + q) - 20, & \text{if } \alpha = 1, \\ 21pq - 2.0004(p + q) + 1.6254, & \text{if } \alpha = -1, \\ 191.1936pq + (1.01364)(p + q) - 2.18524, & \text{if } \alpha = \frac{1}{2}, \\ 42.14298pq - 2.37928(p + q) + 1.732836, & \text{if } \alpha = -\frac{1}{2}. \end{cases} \tag{12}$$

Proof. We consider $G(p, q)$ and formula to compute the results

$$\widehat{\mathfrak{R}}\mathfrak{R}_{\alpha}(G) = \sum_{pq \in X(G)} [\widehat{\mathfrak{R}}_{\chi}(p) \times \widehat{\mathfrak{R}}_{\chi}(q)]^{\alpha}; \quad \alpha = 1, -1, \frac{1}{2}, -\frac{1}{2} \tag{13}$$

For $\alpha = 1$,

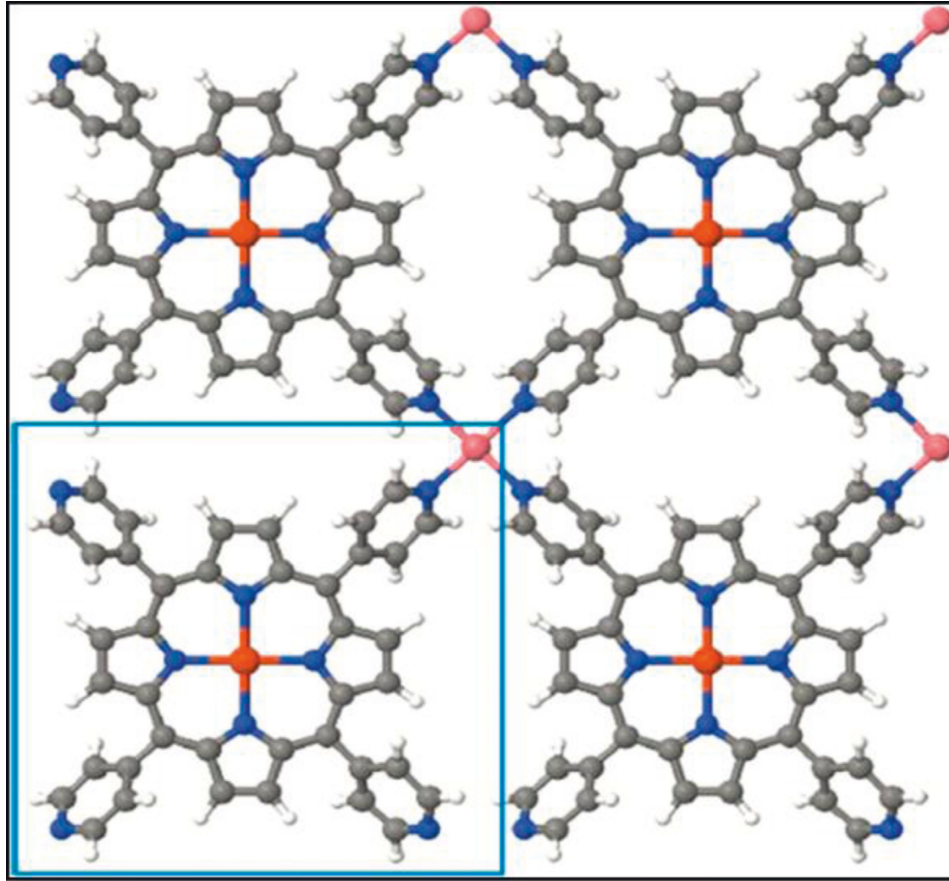
FIGURE 1: 2×2 supercell of M1TPyP-M2 MOFs (M1, M2=Fe and Co).

TABLE 1: Edge partition of M1TPyP-M2 MOFs.

$(\chi(p), \chi(q))$	Number of edges
(1, 3)	$24pq + 1$
(2, 3)	$6p + 6q - 6$
(3, 3)	$56pq - 4p - 4q + 2$
(3, 4)	$8pq - 4p - 4q + 4$

TABLE 2: Reverse-based edge partition of M1TPyP-M2 MOFs.

$(\widehat{\mathfrak{R}}\chi(p), \widehat{\mathfrak{R}}\chi(q))$	Number of edges
(4, 2)	$24pq + 1$
(3, 2)	$6p + 6q - 6$
(2, 2)	$56pq - 4p - 4q + 2$
(2, 1)	$8pq - 4p - 4q + 4$

$$\begin{aligned}
 \widehat{\mathfrak{R}}\mathfrak{R}_1(G) &= \sum_{pq \in \widehat{X}(G)} [\widehat{\mathfrak{R}}\chi(p) \times \widehat{\mathfrak{R}}\chi(q)]^1 \\
 &= (24pq + 1)(4 \times 2) + (6p + 6q - 6)(3 \times 2) + (56pq - 4p - 4q + 2)(2 \times 2) \\
 &\quad + (8pq - 4p - 4q + 4)(2 \times 1) = 8(24pq + 1) + 6(6p + 6q - 6) \\
 &\quad + 4(56pq - 4p - 4q + 2) + 2(8pq - 4p - 4q + 4) = 192pq + 8 + 36p \\
 &\quad + 36q - 36 + 224pq - 16p - 16q + 8 + 16pq - 8p - 8q + 8 \\
 &= 416pq + 12(p + q) - 20.
 \end{aligned} \tag{14}$$

For $\alpha = -1$,

$$\begin{aligned}
\widehat{\mathfrak{R}}\mathfrak{R}_{-1}(G) &= \sum_{pq \in X(G)} [\widehat{\mathfrak{R}}\chi(p) \times \widehat{\mathfrak{R}}\chi(q)]^{-1} \\
&= \frac{(24pq + 1)}{4 \times 2} + \frac{(6p + 6q - 6)}{3 \times 2} + \frac{(56pq - 4p - 4q + 2)}{2 \times 2} \\
&\quad + \frac{(8pq - 4p - 4q + 4)}{2 \times 1} = (24pq + 1)(0.125) + (6p + 6q - 6)(0.1666) \\
&\quad + (56pq - 4p - 4q + 2)(0.25) + (8pq - 4p - 4q + 4)(0.5) \\
&= 3pq + 0.125 + 0.9996p + 0.9996q - 0.9996 + 14pq - p - q + 0.5 \\
&\quad + 4pq - 2p - 2q + 2 = 21pq - 2.0004(p + q) + 1.6254.
\end{aligned} \tag{15}$$

For $\alpha = 1/2$,

$$\begin{aligned}
\widehat{\mathfrak{R}}\mathfrak{R}_{1/2}(G) &= \sum_{pq \in X(G)} [\widehat{\mathfrak{R}}\chi(p) \times \widehat{\mathfrak{R}}\chi(q)]^{1/2} \\
&= (24pq + 1)\sqrt{4 \times 2} + (6p + 6q - 6)\sqrt{3 \times 2} \\
&\quad + (56pq - 4p - 4q + 2)\sqrt{2 \times 2} + (8pq - 4p - 4q + 4)\sqrt{2 \times 1} \\
&= (24pq + 1)\sqrt{8} + (6p + 6q - 6)\sqrt{6} + (56pq - 4p - 4q + 2) \\
&\quad \cdot \sqrt{4} + (8pq - 4p - 4q + 4)\sqrt{2} = (24pq + 1)(2.8284) \\
&\quad + (6p + 6q - 6)(2.4494) + (56pq - 4p - 4q + 2)(2) \\
&\quad + (8pq - 4p - 4q + 4)(1.414) \\
&= 67.8816pq + 2.8284 + 14.66964p + 14.66964q - 14.66964 \\
&\quad + 112pq - 8p - 8q + 4 + 11.312pq - 5.656p - 5.656q + 5.656 \\
&= 191.1936pq + (1.01364)(p + q) - 2.18524.
\end{aligned} \tag{16}$$

For $\alpha = -(1/2)$,

$$\begin{aligned}
\widehat{\mathfrak{R}}\mathfrak{R}_{-(1/2)}(G) &= \sum_{pq \in X(G)} [\widehat{\mathfrak{R}}\chi(p) \times \widehat{\mathfrak{R}}\chi(q)]^{-(1/2)} \\
&= \frac{(24pq + 1)}{\sqrt{4 \times 2}} + \frac{(6p + 6q - 6)}{\sqrt{3 \times 2}} + \frac{(56pq - 4p - 4q + 2)}{\sqrt{2 \times 2}} + \frac{(8pq - 4p - 4q + 4)}{\sqrt{2 \times 1}} \\
&= \frac{(24pq + 1)}{\sqrt{8}} + \frac{(6p + 6q - 6)}{\sqrt{6}} + \frac{(56pq - 4p - 4q + 2)}{\sqrt{4}} + \frac{(8pq - 4p - 4q + 4)}{\sqrt{2}} \\
&= \frac{(24pq + 1)}{2.8284} + \frac{(6p + 6q - 6)}{2.4494} + \frac{(56pq - 4p - 4q + 2)}{2} + \frac{(8pq - 4p - 4q + 4)}{1.414} \\
&= (24pq + 1)(0.353556) + (6p + 6q - 6)(0.40826) + (56pq - 4p - 4q + 2) \\
&\quad \cdot (0.5) + (8pq - 4p - 4q + 4)(0.70721) = 8.4853pq + 0.353556 \\
&\quad + 2.44956p + 2.44956q - 2.44956 + 28pq - 2p - 2q + 1 + 5.65768pq \\
&\quad - 2.82884p - 2.82884q + 2.82884 = 42.14298pq - 2.37928(p + q) + 1.732836.
\end{aligned} \tag{17}$$

□

Theorem 2. We consider the graph $G(p, q)$, then the reverse Atom Bond Connectivity index is equal to $\widehat{\mathfrak{R}}ABC(G) = 62.2248pq - 1.4142(p + q) + 0.7071$.

Proof. We consider $G(p, q)$ and formula to compute the results

$$\begin{aligned}
 \widehat{\mathfrak{R}}ABC(G) &= \sum_{pq \in X(G)} \sqrt{\frac{\widehat{\mathfrak{R}}\chi(p) + \widehat{\mathfrak{R}}\chi(q) - 2}{\widehat{\mathfrak{R}}\chi(p) \times \widehat{\mathfrak{R}}\chi(q)}} \\
 &= (24pq + 1) \sqrt{\frac{4+2-2}{4 \times 2}} + (6p + 6q - 6) \sqrt{\frac{3+2-2}{3 \times 2}} + (56pq - 4p - 4q + 2) \\
 &\quad \cdot \sqrt{\frac{2+2-2}{2 \times 2}} + (8pq - 4p - 4q + 4) \sqrt{\frac{2+1-2}{2 \times 1}} \\
 &= (24pq + 1) \sqrt{\frac{4}{8}} + (6p + 6q - 6) \sqrt{\frac{3}{6}} + (56pq - 4p - 4q + 2) \sqrt{\frac{1}{2}} + (8pq - 4p - 4q + 4) \sqrt{\frac{1}{2}} \quad (18) \\
 &= (24pq + 1)(0.70710) + (6p + 6q - 6)(0.70710) + (56pq - 4p - 4q + 2) \\
 &\quad \cdot (0.70710) + (8pq - 4p - 4q + 4)(0.70710) = 16.9704pq + 0.70710 \\
 &\quad + (p + q - 1)(4.2426) + 39.5976pq - 2.8284p \\
 &\quad - 2.8284q + 1.4142 + 5.6568pq - 2.8284p - 2.8284q + 2.8284 \\
 &= 62.2248pq - 1.4142(p + q) + 0.7071.
 \end{aligned}$$

Theorem 3. We consider the graph $G(p, q)$, then the reverse Geometric Arithmetic index is equal to $\widehat{\mathfrak{R}}GA(G) = 86.169672pq - 1.892466(p + q) + (0.835266)$.

Proof. We consider $G(p, q)$ and formula to compute the results

$$\begin{aligned}
 \widehat{\mathfrak{R}}GA(G) &= \sum_{pq \in X(G)} \frac{2\sqrt{\widehat{\mathfrak{R}}\chi(p) \times \widehat{\mathfrak{R}}\chi(q)}}{\widehat{\mathfrak{R}}\chi(p) + \widehat{\mathfrak{R}}\chi(q)} \\
 &= (24pq + 1) \left[\frac{2\sqrt{4 \times 2}}{4 + 2} \right] + (6p + 6q - 6) \left[\frac{2\sqrt{3 \times 2}}{3 + 2} \right] + (56pq - 4p - 4q + 2) \\
 &\quad \cdot \left[\frac{2\sqrt{2 \times 2}}{2 + 2} \right] + (8pq - 4p - 4q + 4) \left[\frac{2\sqrt{2 \times 1}}{2 + 1} \right] = (24pq + 1) \left[\frac{2\sqrt{8}}{6} \right] + (6p + 6q - 6) \\
 &\quad \cdot \left[\frac{2\sqrt{6}}{5} \right] + (56pq - 4p - 4q + 2) \left[\frac{2 \times 2}{4} \right] + (8pq - 4p - 4q + 4) \left[\frac{2\sqrt{2}}{3} \right] \quad (19) \\
 &= (24pq + 1)(0.9428) + (p + q - 1)(5.87877) \\
 &\quad + (56pq - 4p - 4q + 2) + (8pq - 4p - 4q + 4)(0.942809) \\
 &= 22.6272pq + 0.9428 + 5.87877p + 5.87877q - 5.87877 \\
 &\quad + 56pq - 4p - 4q + 2 + 7.542472pq - 3.771236p - 3.771236q \\
 &\quad + 3.771236 = 86.169672pq - 1.892466(p + q) + (0.835266).
 \end{aligned}$$

Theorem 4. We consider the graph $G(p, q)$, then the reverse First Zagreb index is equal to $\mathfrak{R}M_1(G) = 392pq + 2(p + q) - 4$.

Proof. We consider $G(p, q)$ and formula to compute the results

$$\begin{aligned} \widehat{\mathfrak{R}}M_1(G) &= \sum_{pq \in X(G)} (\widehat{\mathfrak{R}}\chi(p) + \widehat{\mathfrak{R}}\chi(q)) \\ &= (24pq + 1)(4 + 2) + (6p + 6q - 6)(3 + 2) \\ &\quad + (56pq - 4p - 4q + 2)(2 + 2) + (8pq - 4p - 4q + 4)(2 + 1) \\ &= (24pq + 1)(6) + (6p + 6q - 6)(5) + (56pq - 4p - 4q + 2) \\ &\quad \cdot (4) + (8pq - 4p - 4q + 4)(3) = 144pq + 6 + 30p + 30q - 30 \\ &\quad + 224pq - 16p - 16q + 8 + 24pq - 12p - 12q + 12 \\ &= 392pq + 2(p + q) - 4. \end{aligned} \tag{20}$$

Theorem 5. We consider the graph $G(p, q)$, then the reverse Second Zagreb index is equal to $\mathfrak{R}M_2(G) = 432pq + 12(p + q) - 12$.

Proof. We consider $G(p, q)$ and formula to compute the results

$$\begin{aligned} \widehat{\mathfrak{R}}M_2(G) &= \sum_{pq \in X(G)} (\widehat{\mathfrak{R}}\chi(p) \times \widehat{\mathfrak{R}}\chi(q)) \\ &= (24pq + 1)(4 \times 2) + (6p + 6q - 6)(3 \times 2) + (56pq - 4p - 4q + 2)(2 \times 2) \\ &\quad + (8pq - 4p - 4q + 4)(2 \times 1) = (24pq + 1)(8) + (6p + 6q - 6)(6) \\ &\quad + (56pq - 4p - 4q + 2)(4) + (8pq - 4p - 4q + 4)(2) \\ &= 192pq + 8 + 36p + 36q - 36 + 224pq \\ &\quad - 16p - 16q + 8 + 16pq - 8p - 8q + 8 = 432pq + 12(p + q) - 12. \end{aligned} \tag{21}$$

Theorem 6. We consider the graph $G(p, q)$, then the reverse first Zagreb co-index is equal to $\mathfrak{R}\overline{M}_1(G) = 12604pq - 296pq(p + q) + 2(p + q) + 2$.

Proof. We consider $G(p, q)$ and formula to compute the results

$$\begin{aligned} \widehat{\mathfrak{R}}\overline{M}_1(G) &= 2|X(G)|(|V(G)| - 1) - \widehat{\mathfrak{R}}M_1(G) \\ &= 2(88pq - 2p - 2q + 1)(74pq - 1) - [392pq + 2(p + q) - 4] \\ &= 13024pq - 176pq - 296p^2q + 4p - 296pq^2 + 4p \\ &\quad + 148pq - 2 - 392pq - 2p - 2q + 4 \\ &= 12604pq - 296pq(p + q) + 2(p + q) + 2. \end{aligned} \tag{22}$$

Theorem 7. We consider the graph $G(p, q)$, then the reverse Second Zagreb Co-index is equal to $\widehat{\mathfrak{R}}\overline{M}_2(G) = 15488p^2q^2 - 8(p^2 + q^2) - 628pq - 13(p + q) + 16$.

Proof. We consider $G(p, q)$ and formula to compute the results

$$\begin{aligned} \widehat{\mathfrak{R}}\overline{M}_2(G) &= 2|X(G)|^2 - \frac{1}{2}\widehat{\mathfrak{R}}M_1(G) - \widehat{\mathfrak{R}}M_2(G) \\ &= 2(88pq - 2p - 2q + 1)^2 - \frac{1}{2}(392pq + 2(p + q) - 4) \\ &\quad - (432pq + 12(p + q) - 12) = 15488p^2q^2 - 8p^2 - 8q^2 + 2 - 196pq \\ &\quad - p - q + 2 - 432pq - 12p - 12q + 12 = 15488p^2q^2 - 8(p^2 + q^2) \\ &\quad - 628pq - 13(p + q) + 16. \end{aligned} \tag{23}$$

Theorem 8. We consider the graph $G(p, q)$, then the reverse hyper Zagreb index is equal to $\widehat{\mathfrak{R}}HM(G) = 1832pq + 50(p + q) - 46$.

Proof. We consider $G(p, q)$ and formula to compute the results

$$\begin{aligned} \widehat{\mathfrak{R}}HM(G) &= \sum_{pq \in X(G)} [\widehat{\mathfrak{R}}\chi(p) + \widehat{\mathfrak{R}}\chi(q)]^2 \\ &= (24pq + 1)(4 + 2)^2 + (6p + 6q - 6)(3 + 2)^2 + (56pq - 4p - 4q + 2) \\ &\quad \cdot (2 + 2)^2 + (8pq - 4p - 4q + 4)(2 + 1)^2 = (24pq + 1)(36) + (6p + 6q - 6) \\ &\quad \cdot (25) + (56pq - 4p - 4q + 2)(16) + (8pq - 4p - 4q + 4)(9) \\ &= 864pq + 36 + 150p + 150q - 150 + 896pq - 64p - 64q + 32 \\ &\quad + 73pq - 36p - 36q + 36 = 1832pq + 50(p + q) - 46. \end{aligned} \tag{24}$$

Theorem 9. We consider the graph $G(p, q)$, then the reverse forgotten index is equal to $\widehat{\mathfrak{R}}F(G) = 968pq + 26(p + q) - 22$.

Proof. We consider $G(p, q)$ and formula to compute the results

$$\begin{aligned} \widehat{\mathfrak{R}}F(G) &= \sum_{pq \in X(G)} [\widehat{\mathfrak{R}}\chi(p)^2 + \widehat{\mathfrak{R}}\chi(q)]^2 \\ &= (24pq + 1)(4^2 + 2^2) + (6p + 6q - 6)(3^2 + 2^2) + (56pq - 4p - 4q + 2) \\ &\quad \cdot (2^2 + 2^2) + (8pq - 4p - 4q + 4)(2^2 + 1^2) \\ &= (24pq + 1)(20) + (6p + 6q - 6)(13) + (56pq - 4p - 4q + 2)(8) \\ &\quad + (8pq - 4p - 4q + 4)(5) = 968pq + 20 + 78p + 78q - 78 - 32p \\ &\quad - 32q + 16 - 20p - 20q + 20 = 968pq + 26(p + q) - 22. \end{aligned} \tag{25}$$

Theorem 10. We consider the graph $G(p, q)$, then the reverse Balaban index is equal to $\widehat{\mathfrak{R}}J(G) = (88pq - 2(p + q) + 1/14pq - 2(p + q) + 3)[42.14298pq - 2.37928(p + q) + 1.732836]$

Proof. We consider $G(p, q)$ and formula to compute the results

Here, p denotes the size and q denotes the order of graph.

$$\begin{aligned} \widehat{\mathfrak{R}}J(G) &= \frac{p}{p-q+2} \sum_{pq \in X(G)} \frac{1}{\sqrt{\widehat{\mathfrak{R}}\chi(p) \times \widehat{\mathfrak{R}}\chi(q)}} \\ &= \frac{88pq - 2p - 2q + 1}{(88pq - 2p - 2q + 1) - 74pq + 2} \left[\frac{24pq + 1}{\sqrt{4 \times 2}} + \frac{6c + 6d - 6}{\sqrt{3 \times 2}} \right. \\ &\quad \left. + \frac{56pq - 4p - 4q + 2}{\sqrt{2 \times 2}} + \frac{8pq - 4p - 4q + 4}{\sqrt{2 \times 1}} \right] = \frac{88pq - 2p - 2q + 1}{(88pq - 2p - 2q + 1) - 74pq + 2} \quad (26) \\ &\cdot [42.14298pq - 2.37928(p + q) + 1.732836] = \frac{88pq - 2(p + q) + 1}{14pq - 2(p + q) + 3} \\ &\cdot [42.14298pq - 2.37928(p + q) + 1.732836]. \end{aligned}$$

Theorem 11. We consider the graph $G(p, q)$, then the reverse first multiple Zagreb index is equal to

$$\widehat{\mathfrak{R}}PM_1(G) = 17280 \left[\begin{array}{l} 48p^4q(28q^2 - 16q + 1) + 2p^3(672q^4 - 1440q^3 + 844q^2 - 76q + 1) \\ + p^2(-768q^4 + 1688q^3 - 1080q^2 + 164q - 5) + 4p(q - 1)^2 \\ (12q^2 - 14q + 1) + (p - 1)^2(2q - 1) \end{array} \right]. \quad (27)$$

Proof. We consider $G(p, q)$ and formula to compute the results

$$\begin{aligned} \widehat{\mathfrak{R}}PM_1(G) &= \prod_{pq \in X(G)} [\widehat{\mathfrak{R}}\chi(p) + \widehat{\mathfrak{R}}\chi(q)] \\ &= (24pq + 1)(4 + 2) + (6p + 6q - 6)(3 + 2) + (56pq - 4p - 4q + 2) \\ &\quad \cdot (2 + 2) + (8pq - 4p - 4q + 4)(2 + 1) = (24pq + 1)(6) + (6p + 6q - 6)(5) + (56pq - 4p - 4q + 2)(4) \\ &\quad + (8pq - 4p - 4q + 4)(3) = 23224320p^4q^3 - 13271040p^4q^2 + 829440p^4q + 23224320p^3q^4 \\ &\quad - 49766400p^3q^3 + 29168640p^3q^2 - 2626560p^3q + 34560p^3 \\ &\quad - 13271040p^2q^4 + 29168640p^2q^3 - 18662400p^2q^2 + 2833920p^2q \quad (28) \\ &\quad - 86400p^2 + 829440pq^4 - 2626560pq^3 + 2833920pq^2 - 1105920pq \\ &\quad + 69120p + 34560q^3 - 86400q^2 + 69120q - 17280 \\ &= 17280 \left[\begin{array}{l} 48p^4q(28q^2 - 16q + 1) + 2p^3(672q^4 - 1440q^3 + 844q^2 - 76q + 1) \\ + p^2(-768q^4 + 1688q^3 - 1080q^2 + 164q - 5) + 4p(q - 1)^2 \\ \cdot (12q^2 - 14q + 1) + (p - 1)^2(2q - 1) \end{array} \right]. \end{aligned}$$

Theorem 12. We consider the graph $G(p, q)$, then the reverse second multiple Zagreb index is equal to

$$\widehat{\mathfrak{R}}PM_2(G) = 18432[48p^4q(28q^2 - 16q + 1) + 2p^3(672q^4 - 1440q^3 + 844q^2 - 76q + 1) + p^2(-768q^4 + 1688q^3 - 1080q^2 + 164q - 5) + 4p(q - 1)^2(12q^2 - 14q + 1) + (p - 1)^2(2q - 1)].$$

Proof. We consider $G(p, q)$ and formula to compute the results

$$\begin{aligned}
 \widehat{\mathfrak{R}}\text{PM}_2(G) &= \prod_{pq \in X(G)} [\widehat{\mathfrak{R}}\chi(p) \times \widehat{\mathfrak{R}}\chi(q)] \\
 &= (24pq + 1)(4 \times 2) + (6p + 6q - 6)(3 \times 2) + (56pq - 4p - 4q + 2) \\
 &\quad \cdot (2 \times 2) + (8pq - 4p - 4q + 4)(2 \times 1) \\
 &= (24pq + 1)(8) + (6p + 6q - 6)(6) + (56pq - 4p - 4q + 2)(4) \\
 &\quad + (8pq - 4p - 4q + 4)(2) = 24772608p^4q^3 - 14155776p^4q^2 + 884736p^4q \\
 &\quad + 24772608p^3q^4 - 53084160p^3q^3 + 31113216p^3q^2 - 2801664p^3q + 34864p^3 \\
 &\quad - 14155776p^2q^4 + 31113216p^2q^3 - 19906560p^2q^2 + 3022848p^2q - 92160p^2 \\
 &\quad + 884736pq^4 - 2801664pq^3 + 3022848pq^2 - 1179648pq + 73728p \\
 &\quad + 36864q^3 - 92160q^2 + 73728q - 18432 \\
 &= 18432 \left[\begin{array}{l} 48p^4q(28q^2 - 16q + 1) + 2p^3(672q^4 - 1440q^3 + 844q^2 - 76q + 1) \\ + p^2(-768q^4 + 1688q^3 - 1080q^2 + 164q - 5) + 4p(q - 1)^2 \\ \cdot (12q^2 - 14q + 1) + (p - 1)^2(2q - 1) \end{array} \right].
 \end{aligned} \tag{29}$$

Theorem 13. We consider the graph $G(p, q)$, then the reverse first redefined Zagreb index is equal to $\mathfrak{R}\mathfrak{ReZG}_1(G) = 86pq - 5(p + q) + 3.75$.

Proof. We consider $G(p, q)$ and formula to compute the results □

$$\begin{aligned}
 \widehat{\mathfrak{R}}\mathfrak{ReZG}_1(G) &= \sum_{pq \in X(G)} \frac{\widehat{\mathfrak{R}}\chi(p) + \widehat{\mathfrak{R}}\chi(q)}{\widehat{\mathfrak{R}}\chi(p) \times \widehat{\mathfrak{R}}\chi(q)} \\
 &= (24pq + 1) \frac{4 + 2}{4 \times 2} + (6p + 6q - 6) \frac{3 + 2}{3 \times 2} + (56pq - 4p - 4q + 2) \\
 &\quad \cdot \frac{2 + 2}{2 \times 2} + (8pq - 4p - 4q + 4) \frac{2 + 1}{2 \times 1} = (24pq + 1) \frac{6}{8} + (6p + 6q - 6) \\
 &\quad \cdot \frac{5}{6} + (56pq - 4p - 4q + 2) \frac{4}{4} + (8pq - 4p - 4q + 4) \frac{3}{2} \\
 &= 86pq - 5(p + q) + 3.75.
 \end{aligned} \tag{30}$$

□

Theorem 14. We consider the graph $G(p, q)$, then the reverse second redefined Zagreb index is equal to $\mathfrak{RReZG}_2(G) = 93.3253pq + 0.53336(p + q) - 1.20036$.

Proof. We consider $G(p, q)$ and formula to compute the results

$$\begin{aligned} \widehat{\mathfrak{RReZG}}_2(G) &= \sum_{pq \in X(G)} \frac{\widehat{\mathfrak{R}}\chi(p) \times \widehat{\mathfrak{R}}\chi(q)}{\widehat{\mathfrak{R}}\chi(p) + \widehat{\mathfrak{R}}\chi(q)} \\ &= (24pq + 1) \frac{4 \times 2}{4 + 2} + (6p + 6q - 6) \frac{3 \times 2}{3 + 2} + (56pq - 4p - 4q + 2) \\ &\quad \cdot \frac{2 \times 2}{2 + 2} + (8pq - 4p - 4q + 4) \frac{2 \times 1}{2 + 1} \\ &= (24pq + 1) \frac{8}{6} + (6p + 6q - 6) \frac{6}{5} + (56pq - 4p - 4q + 2) \\ &\quad \cdot \frac{4}{4} + (8pq - 4p - 4q + 4) \frac{2}{3} = 93.3253pq + 0.53336(p + q) - 1.20036. \end{aligned} \tag{31}$$

Theorem 15. We consider the graph $G(p, q)$, then the reverse third redefined Zagreb index is equal to $\mathfrak{RReZG}_3(G) = 2096pq + 92(p + q) - 76$.

Proof. We consider $G(p, q)$ and formula to compute the results

$$\begin{aligned} \widehat{\mathfrak{RReZG}}_3(G) &= \sum_{pq \in X(G)} (\widehat{\mathfrak{R}}\chi(p) \times \widehat{\mathfrak{R}}\chi(q)) (\widehat{\mathfrak{R}}\chi(p) + \widehat{\mathfrak{R}}\chi(q)) \\ &= (24pq + 1)(4 \times 2)(4 + 2) + (6p + 6q - 6)(3 \times 2)(3 + 2) \\ &\quad + (56pq - 4p - 4q + 2)(2 \times 2)(2 + 2) + (8pq - 4p - 4q + 4)(2 \times 1)(2 + 1) \\ &= (24pq + 1)(8)(6) + (6p + 6q - 6)(6)(5) + (56pq - 4p - 4q + 2) \\ &\quad \cdot (4)(4) + (8pq - 4p - 4q + 4)(2)(3) = 2096pq + 92(p + q) - 76. \end{aligned} \tag{32}$$

Theorem 16. We consider the graph $G(p, q)$, then the reverse augmented Zagreb index is equal to $\mathfrak{RAZI}(G) = 704pq - 16(p + q) + 8$.

Proof. We consider $G(p, q)$ and formula to compute the results

$$\begin{aligned} \widehat{\mathfrak{RAZI}}(G) &= \sum_{pq \in X(G)} \left(\frac{\widehat{\mathfrak{R}}\chi(p) \times \widehat{\mathfrak{R}}\chi(q)}{\widehat{\mathfrak{R}}\chi(p) \times \widehat{\mathfrak{R}}\chi(q) - 2} \right)^3 \\ &= (24pq + 1) \left(\frac{4 \times 2}{4 + 2 - 2} \right)^3 + (6p + 6q - 6) \left(\frac{3 \times 2}{3 + 2 - 2} \right)^3 \\ &\quad + (56pq - 4p - 4q + 2) \left(\frac{2 \times 2}{2 + 2 - 2} \right)^3 + (8pq - 4p - 4q + 4) \left(\frac{2 \times 1}{2 + 1 - 2} \right)^3 \\ &= (24pq + 1)(8) + (p + q - 1)(6)(8) + (56pq - 4p - 4q + 2)(8) \\ &\quad + (8pq - 4p - 4q + 4)(8) = 704pq - 16(p + q) + 8. \end{aligned} \tag{33}$$

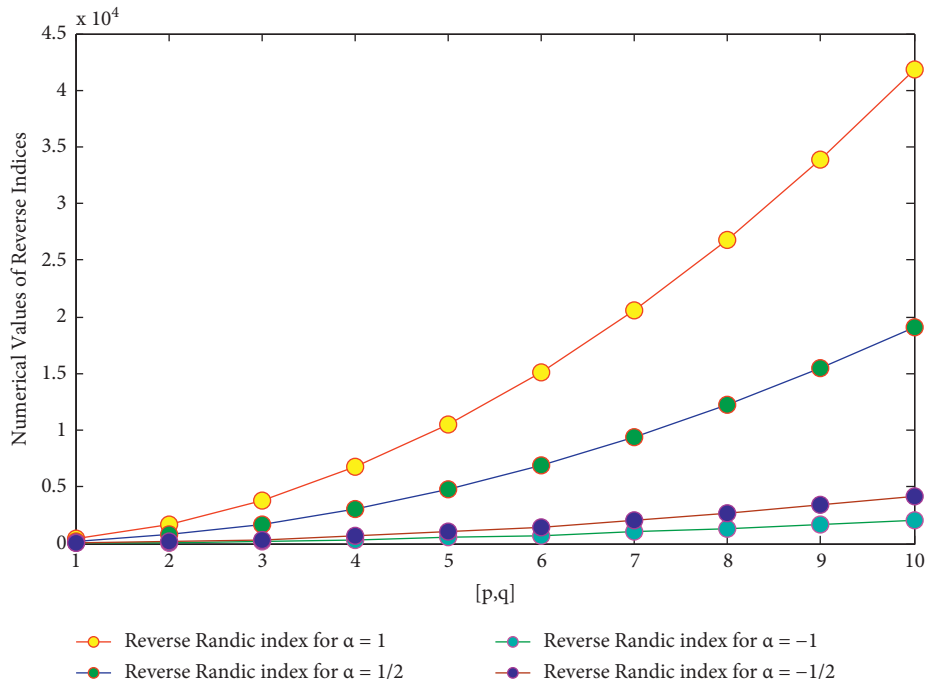


FIGURE 2: Comparison of the reverse Randic index $\widehat{\mathfrak{RR}}_1(G)$, $\widehat{\mathfrak{RR}}_{-1}(G)$, $\widehat{\mathfrak{RR}}_{1/2}(G)$, and $\widehat{\mathfrak{RR}}_{-(1/2)}(G)$.

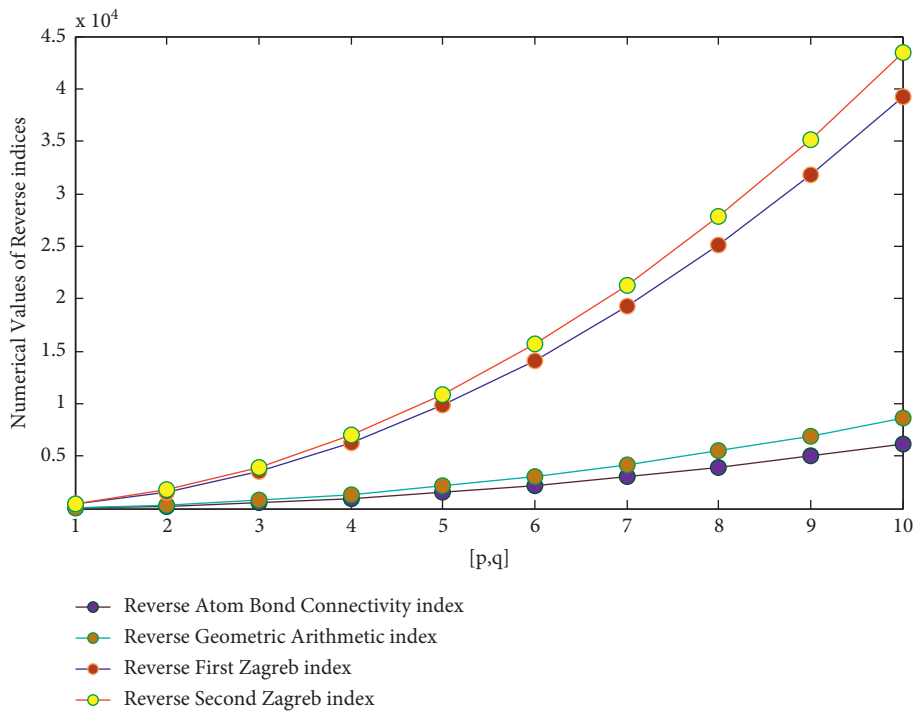


FIGURE 3: Comparison of the reverse atom bond connectivity index $\widehat{\mathfrak{R}}ABC(G)$, the reverse geometric arithmetic index $\widehat{\mathfrak{R}}GA(G)$, the reverse first Zagreb index $\widehat{\mathfrak{R}}M_1(G)$, and the reverse second Zagreb index $\widehat{\mathfrak{R}}M_2(G)$.

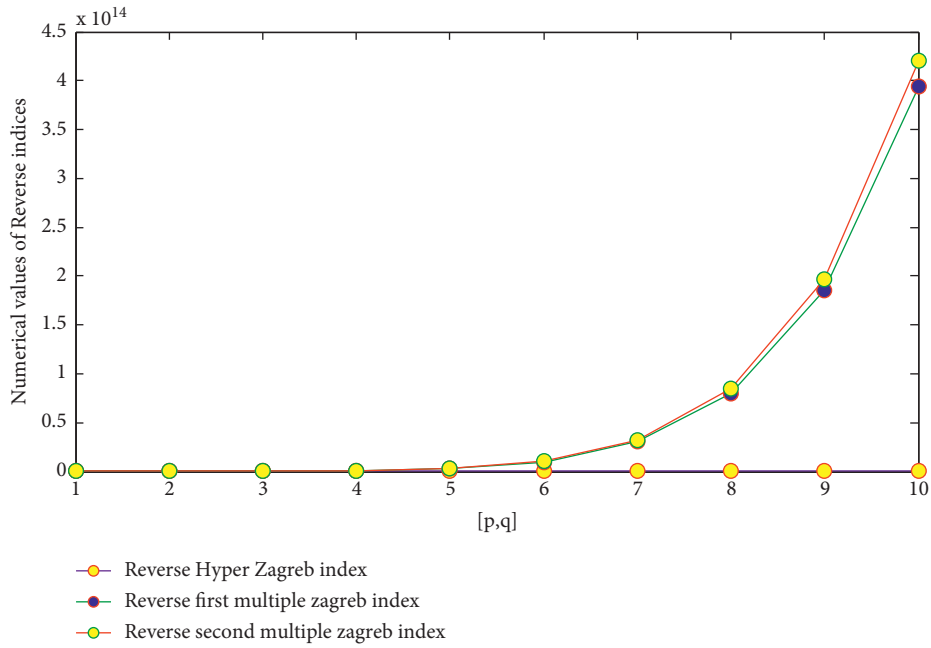


FIGURE 4: Graphical comparison of the reverse hyper Zagreb $\widehat{\mathfrak{R}}\text{HM}(G)$, the reverse first multiple Zagreb index $\widehat{\mathfrak{R}}\text{PM}_1(G)$, and the reverse second multiple Zagreb index $\widehat{\mathfrak{R}}\text{PM}_2(G)$.

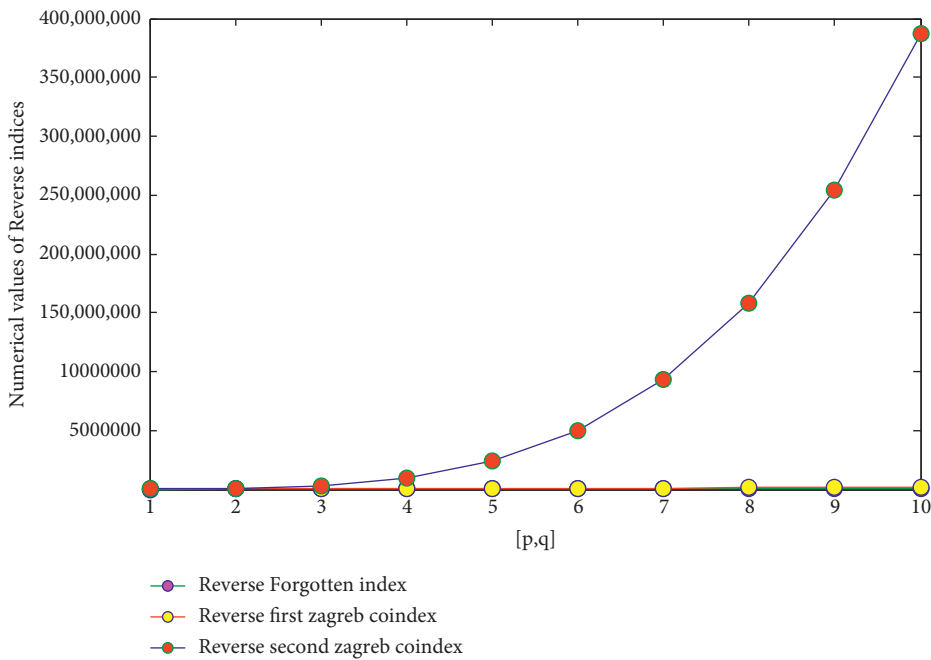


FIGURE 5: Comparison of the reverse forgotten index $\widehat{\mathfrak{R}}F(G)$, the reverse first Zagreb co-index $\widehat{\mathfrak{R}}\overline{M}_1(G)$, and the reverse second Zagreb co-index $\widehat{\mathfrak{R}}\overline{M}_2(G)$.

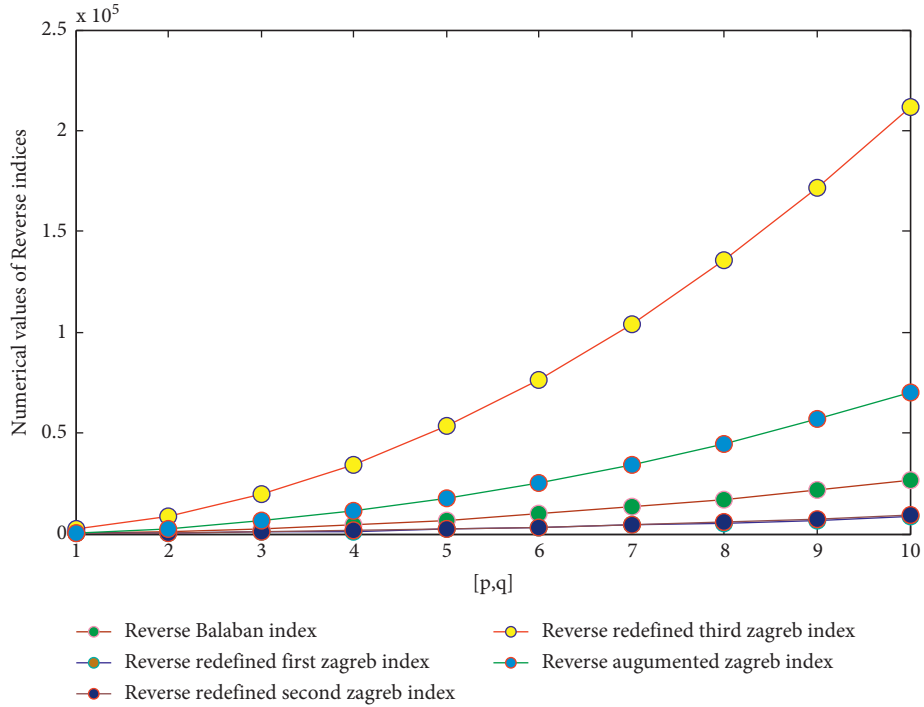


FIGURE 6: Comparison of the reverse Balaban index $\widehat{\mathfrak{R}}J(G)$, the reverse redefined first Zagreb index $\widehat{\mathfrak{R}}\text{ReZG}_1(G)$, the reverse redefined second Zagreb index $\widehat{\mathfrak{R}}\text{ReZG}_2(G)$, the reverse redefined third Zagreb index $\widehat{\mathfrak{R}}\text{ReZG}_3(G)$, and the reverse augmented Zagreb index $\widehat{\mathfrak{R}}\text{AZI}(G)$.

TABLE 3: Numerical comparison of $\widehat{\mathfrak{R}}\mathfrak{N}_1(G)$, $\widehat{\mathfrak{R}}\mathfrak{N}_{-1}(G)$, $\widehat{\mathfrak{R}}\mathfrak{N}_{1/2}(G)$, and $\widehat{\mathfrak{R}}\mathfrak{N}_{-(1/2)}(G)$ for M1TPyP-M2 MOFs.

[p, q]	$\widehat{\mathfrak{R}}\mathfrak{N}_1(G)$	$\widehat{\mathfrak{R}}\mathfrak{N}_{-1}(G)$	$\widehat{\mathfrak{R}}\mathfrak{N}_{1/2}(G)$	$\widehat{\mathfrak{R}}\mathfrak{N}_{-(1/2)}(G)$
[1, 1]	420	18.6174	191.03564	39.117356
[2, 2]	1692	77.6094	766.643	160.7876
[3, 3]	3796	178.623	1724.639	366.743
[4, 4]	6732	321.6222	3065.021	656.986
[5, 5]	10500	506.6214	4787.79	1031.514
[6, 6]	15100	733.6206	6892.94	1490.32
[7, 7]	20532	1002.6198	9380.49212	2033.42
[8, 8]	26796	1313.619	12250.42	2660.815
[9, 9]	33892	1666.6182	15502.741	3372.487
[10, 10]	41820	2061.6174	19137.447	4168.445

TABLE 4: Numerical comparison of $\widehat{\mathfrak{R}}\text{ABC}(G)$, $\widehat{\mathfrak{R}}\text{GA}(G)$, $\widehat{\mathfrak{R}}M_1(G)$, and $\widehat{\mathfrak{R}}M_2(G)$ for M1TPyP-M2 MOFs.

[p, q]	$\widehat{\mathfrak{R}}\text{ABC}(G)$	$\widehat{\mathfrak{R}}\text{GA}(G)$	$\widehat{\mathfrak{R}}M_1(G)$	$\widehat{\mathfrak{R}}M_2(G)$
[1, 1]	60.1035	83.220006	392	444
[2, 2]	243.949	337.94409	1572	1764
[3, 3]	552.24	765.007518	3536	3948
[4, 4]	984.99	1364.41029	6284	6996
[5, 5]	1542.1851	2136.152406	9816	10908
[6, 6]	2223.829	3080.233	14132	15684
[7, 7]	3029.92	4196.6546	19232	21324
[8, 8]	3960.46	5485.4148	25116	27828
[9, 9]	5015.4603	6946.514	31784	35196
[10, 10]	6194.9031	8579.9531	39236	43428

TABLE 5: Numerical comparison of $\widehat{\mathfrak{R}}\text{HM}(G)$, $\widehat{\mathfrak{R}}\text{PM}_1(G)$, and $\widehat{\mathfrak{R}}\text{PM}_2(G)$ for M1TPyP-M2 MOFs.

$[p, q]$	$\widehat{\mathfrak{R}}\text{HM}(G)$	$\widehat{\mathfrak{R}}\text{M}_1(G)$	$\widehat{\mathfrak{R}}\text{PM}_2(G)$
[1, 1]	1886	10800000	1152000
[2, 2]	7482	$2.6400e+09$	$2.8159e+09$
[3, 3]	16742	$5.8740e+10$	$6.2656e+10$
[4, 4]	29666	$5.0412e+11$	$5.3772e+11$
[5, 5]	46254	$2.6097e+12$	$2.7837e+12$
[6, 6]	66506	$9.8791e+12$	$1.0538e+13$
[7, 7]	90422	$3.0228e+13$	$3.2243e+13$
[8, 8]	118002	$7.9277e+13$	$8.4562e+13$
[9, 9]	149246	$1.8500e+14$	$1.9733e+14$
[10, 10]	184154	$3.9394e+14$	$4.2021e+14$

TABLE 6: Numerical comparison of $\widehat{\mathfrak{R}}F(G)$, $\widehat{\mathfrak{R}}\overline{M}_1(G)$, and $\widehat{\mathfrak{R}}\overline{M}_2(G)$ for M1TPyP-M2 MOFs.

$[p, q]$	$\widehat{\mathfrak{R}}F(G)$	$\widehat{\mathfrak{R}}\overline{M}_1(G)$	$\widehat{\mathfrak{R}}\overline{M}_2(G)$
[1, 1]	998	12018	14834
[2, 2]	3954	45690	245196
[3, 3]	8846	97466	1248670
[4, 4]	15674	163794	3954536
[5, 5]	24438	241122	9663786
[6, 6]	35138	325898	20049124
[7, 7]	47774	414570	37154966
[8, 8]	62346	503586	63397440
[9, 9]	78854	589394	101564386
[10, 10]	97298	668442	154815356

TABLE 7: Numerical comparison of $\widehat{\mathfrak{R}}J(G)$, $\widehat{\mathfrak{R}}\text{AZI}(G)$, $\widehat{\mathfrak{R}}\text{ReZG}_1(G)$, $\widehat{\mathfrak{R}}\text{ReZG}_2(G)$, and $\widehat{\mathfrak{R}}\text{ReZG}_3(G)$ for M1TPyP-M2 MOFs.

$[p, q]$	$\widehat{\mathfrak{R}}J(G)$	$\widehat{\mathfrak{R}}\text{AZI}(G)$	$\widehat{\mathfrak{R}}\text{ReZG}_1(G)$	$\widehat{\mathfrak{R}}\text{ReZG}_2(G)$	$\widehat{\mathfrak{R}}\text{ReZG}_3(G)$
[1, 1]	255.7667	680	79.7500	93.1917	2204
[2, 2]	$1.8077e+03$	2760	327.7500	374.2343	8676
[3, 3]	$2.4481e+03$	6248	747.7500	841.9275	19340
[4, 4]	$4.3374e+03$	11144	$1.3398e+03$	$1.4963e+03$	34196
[5, 5]	$6.7560e+03$	17448	$2.1038e+03$	$2.3373e+03$	53244
[6, 6]	$9.7041e+03$	25160	$3.0398e+03$	$3.3649e+03$	76484
[7, 7]	$1.3182e+04$	34280	$4.1478e+03$	$4.5792e+03$	103916
[8, 8]	$1.7189e+04$	44808	$5.4278e+03$	$5.9802e+03$	135540
[9, 9]	$2.1727e+04$	56744	$6.8798e+03$	$7.5677e+03$	171356
[10, 10]	$2.6794e+04$	70088	$8.5038e+03$	$9.3420e+03$	211364

3. Numerical and Graphical Representation of M1TPyP-M2 MOFs (M1, M2 = Fe and Co)

Here, we compute the numerical results for topological indices for M1TPyP-M2 MOFs to observe the relationship between statistical and biological behaviour. We have applied equal values of p and q to calculate the reverse degree based indices. Furthermore, we have drawn Figures 2–6 for the structure of M1TPyP-M2 MOFs to examine the graphical behaviour of topological indices calculated above to speculate physiochemical and biological properties. It can be perceived from Tables 3–7 that all topological indices calculated for the structures of M1TPyP-M2 MOFs increase with the increase in p and q . It has been observed clearly from the figures that all indices are in an ascending order as

the value of p and q is increasing gradually. Thus, the increasing trend shows that the values of topological indices are increasing accordingly in Tables 3–7.

4. Conclusion

In the investigation of the quantitative structure property relationships (QSPRs) and (QSARs), topological descriptors are very important tools to estimate and establish the main characteristics of the bioactivity and chemical compounds. In this article, we have provided the results on reverse degree based topological indices as given in Figures 2–6 for M1TPyP-M2 MOFs; furthermore, indices showed increased values for M1TPyP-M2 MOFs. This computational methodology will develop the investigators to recognise the

preferred model more easily and would inspire the researchers to focus on the organic framework. The method of computation discussed here is very beneficial to evaluate the physicochemical properties of the stated framework and is cost-effective and time-efficient.

Data Availability

All data required for this research work are included within the manuscript.

Conflicts of Interest

The authors declare no conflicts of interest.

Acknowledgments

The corresponding author thank the International Science Program (ISP) in Uppsala, Sweden, for the financial support he got via the capacity building project of the Department of Mathematics, Addis Ababa University.

References

- [1] Y. M. Chu, M. Abid, M. I. Qureshi, A. Fahad, and A. Aslam, "Irregular topological indices of certain metal organic frameworks," *Main Group Metal Chemistry*, vol. 44, no. 1, pp. 73–81, 2021.
- [2] P. Xu, M. Azeem, M. M. Izhar, S. M. Shah, M. A. Binyamin, and A. Aslam, "On topological descriptors of certain metal-organic frameworks," *Journal of Chemistry*, vol. 2020, Article ID 8819008, 12 pages, 2020.
- [3] Y. Kinoshita, I. Matsubara, T. Higuchi, and Y. Saito, "The crystal structure of bis (adiponitrilo) copper (I) nitrate," *Bulletin of the Chemical Society of Japan*, vol. 32, no. 11, pp. 1221–1226, 1959.
- [4] B. F. Hoskins and R. Robson, "Infinite polymeric frameworks consisting of three dimensionally linked rod- like segments," *Journal of the American Chemical Society*, vol. 111, no. 15, pp. 5962–5964, 1989.
- [5] J. Lee, O. K. Farha, J. Roberts, K. A. Scheidt, S. T. Nguyen, and J. T. Hupp, "Metal-organic framework materials as catalysts," *Chemical Society Reviews*, vol. 38, no. 5, pp. 1450–1459, 2009.
- [6] P. Horcajada, C. Serre, G. Maurin et al., "Flexible porous metal-organic frameworks for a controlled drug delivery," *Journal of the American Chemical Society*, vol. 130, no. 21, pp. 6774–6780, 2008.
- [7] L. J. Murray, M. Dinca, and J. R. Long, "Hydrogen storage in metal-organic frameworks," *Chemical Society Reviews*, vol. 38, no. 5, pp. 1294–1314, 2009.
- [8] T. K. Warren, R. Jordan, M. K. Lo et al., "Therapeutic efficacy of the small molecule GS-5734 against ebola virus in rhesus monkeys," *Nature*, vol. 531, no. 7594, pp. 381–385, 2016.
- [9] I. Garcia, Y. Fall, and G. Gomez, "Using topological indices to predict anti-alzheimer and anti-parasitic GSK-3 inhibitors by multi-target QSAR in silico screening," *Molecules*, vol. 15, no. 8, pp. 5408–5422, 2010.
- [10] B. Furtula, A. Graovac, and D. Vukicevic, "Augmented Zagreb index," *Journal of Mathematical Chemistry*, vol. 48, no. 2, pp. 370–380, 2010.
- [11] P. Ali, S. A. K. Kirmani, O. Al Rugaie, and F. Azam, "Degree-based topological indices and polynomials of hyaluronic acid-curcumin conjugates," *Saudi Pharmaceutical Journal*, vol. 28, no. 9, pp. 1093–1100, 2020.
- [12] M. Kamran, N. Salamat, R. H. Khan, U. Ur Rehman Asghar, M. A. Alam, and M. K. Pandit, "Computation of M-polynomial and topological indices of phenol formaldehyde," *Journal of Chemistry*, vol. 2022, pp. 1–11, 2022.
- [13] S. Wazzan and A. Saleh, "Locating and multiplicative locating indices of graphs with QSPR analysis," *Journal of Mathematics*, vol. 2021, pp. 1–15, 2021.
- [14] R. Todeschini and V. Consonni, *Handbook of Molecular Descriptors, Methods and Principles in Medicinal Chemistry*, Wiley, New Jersey, USA, 2000.
- [15] H. Wiener, "Structural determination of paraffin boiling points," *Journal of the American Chemical Society*, vol. 69, no. 1, pp. 17–20, 1947.
- [16] I. Gutman and N. Trinajstić, "Graph theory and molecular orbitals. Total pi-electron energy of alternant hydrocarbons," *Chemical Physics Letters*, vol. 17, no. 4, pp. 535–538, 1972.
- [17] M. Randić, "Characterization of molecular branching," *Journal of the American Chemical Society*, vol. 97, no. 23, pp. 6609–6615, 1975.
- [18] X. Wang, Z. Lin, and L. Miao, "Degree based topological indices of product graphs," *Open Journal of Discrete Applied Mathematics*, vol. 4, no. 3, pp. 60–71, 2021.
- [19] O. C. Havare, "The inverse sum indeg index $\chi^*(G)$ and $\chi^*(G)$ energy of Hyaluronic Acid-Paclitaxel molecules used in anticancer drugs," *Open Journal of Discrete Applied Mathematics*, vol. 4, no. 3, pp. 72–81, 2021.
- [20] P. V. Patil and G. G. Yattinahalli, "Second Zagreb indices of transformation graphs and total transformation graphs," *Open Journal of Discrete Applied Mathematics*, vol. 3, no. 1, pp. 1–7, 2020.
- [21] H. Ali and A. Sajjad, "On further results of hex derived networks," *Open Journal of Discrete Applied Mathematics*, vol. 2, no. 1, pp. 32–40, 2019.
- [22] V. R. Kulli, "Reverse Zagreb and reverse hyper-Zagreb indices and their polynomials of rhombus silicate networks," *Annals of Pure and Applied Mathematics*, vol. 16, no. 1, pp. 47–51, 2018.
- [23] J. Wei, M. Cancan, A. U. Rehman et al., "On topological indices of Remdesivir compound used in treatment of corona virus (COVID 19)," *Polycyclic Aromatic Compounds*, vol. 2021, 2021.
- [24] D. Zhao, Y.-M. Chu, M. K. Siddiqui et al., "On reverse degree based topological indices of polycyclic metal organic network," *Polycyclic Aromatic Compounds*, vol. 2021, pp. 1–18, 2021.
- [25] C. Y. Jung, M. A. Gondal, N. Ahmad, and S. M. Kang, "Reverse degree based indices of some nanotubes," *Journal of Discrete Mathematical Sciences and Cryptography*, vol. 22, no. 7, pp. 1289–1294, 2019.
- [26] Y. C. Kwun, A. U. R. Virk, M. Rafaqat, M. U. Rehman, and W. Nazeer, "Some reversed degree-based topological indices

- for graphene,” *Journal of Discrete Mathematical Sciences and Cryptography*, vol. 22, no. 7, pp. 1305–1314, 2019.
- [27] A. J. M. Khalaf, A. U. R. Virk, A. Ali, and M. Cancan, *Journal of Prime Research in Mathematics*, vol. 17, no. 1, 40 pages, 2021.
- [28] M. S. Rosary, “Topological study of line graph of Remdesivir compound used in the treatment of corona virus,” *Polycyclic Aromatic Compounds*, vol. 2021, pp. 1–17, 2021.
- [29] J. B. Liu and M. Rosary, “Topological analysis of para line graph of Remdesivir used in the prevention of corona virus,” *International Journal of Quantum Chemistry*, vol. 121, 2021.
- [30] E. Estrada, L. Torres, L. Rodriguez, and I. Gutman, “An atom-bond connectivity index: modelling the enthalpy of formation of alkanes,” *Indian Journal of Chemistry, Section A: Inorganic, Physical, Theoretical & Analytical*, vol. 37, no. 10, pp. 849–855, 1998.
- [31] D. Vukicevic and B. Furtula, “Topological index based on the ratios of geometrical and arithmetical means of end-vertex degrees of edges,” *Journal of Mathematical Chemistry*, vol. 46, no. 4, pp. 1369–1376, 2009.
- [32] B. Furtula and I. Gutman, “A forgotten topological index,” *Journal of Mathematical Chemistry*, vol. 53, no. 4, pp. 1184–1190, 2015.
- [33] T. Doslic, “Vertex-weighted Wiener polynomials for composite graphs,” *Ars Mathematica Contemporanea*, vol. 1, no. 1, pp. 66–80, 2008.
- [34] I. Gutman, B. Furtula, Z. K. Vukicevic, and G. Popivoda, “On Zagreb indices and coindices,” *MATCH Communications in Mathematical and in Computer Chemistry*, vol. 74, no. 1, pp. 5–16, 2015.
- [35] G. H. Shirdel, H. Rezapour, and A. M. Sayadi, “The hyper-Zagreb index of graph operations, Iran,” *Journal of Mathematical Chemistry*, vol. 4, no. 2, pp. 213–220, 2013.
- [36] B. Furtula and I. Gutman, “A forgotten topological index,” *Journal of Mathematical Chemistry*, vol. 53, no. 4, pp. 1184–1190, 2015.
- [37] P. S. Ranjini, V. Lokesha, and A. Usha, “Relation between phenylene and hexagonal squeeze using harmonic index,” *International Journal of Graph Theory*, vol. 1, no. 4, pp. 116–121, 2013.